ISSN: 0974-5823 Vol. 7 No. 1 January, 2022

International Journal of Mechanical Engineering

On the Issue of Precision of Laser Triangulation Rangefinders *

Filonov Ivan Vladimirovich

Postgraduate student,

Federal Autonomous Educational Institution of Higher Education Far Eastern Federal University, Vladivostok

Notkin Boris Sergeevich

Ph.D. in engineering, Associate Professor,

Institute of Automation and Control Processes far Eastern Branch of the Russian Academy of Sciences, Vladivostok

Zmeu Konstantin Vitalyevich

Ph.D. in engineering, Associate Professor,

Federal Autonomous Educational Institution of Higher Education Far Eastern Federal University, Vladivostok

Abstract The paper covers a class of laser triangulation measurement systems based on a laser and a camera. Such systems are widely applied in practical tasks, with the range and accuracy of distance measurement being primary features. The article identifies and investigates the design parameters of the measuring system which determine its range, demonstrates their variability and impact on the distribution of sensitivity. As the study reveals, the key role in this impact is played by the ratio of the boundary values of the operating range. A quantitative criterion for assessing the uniformity of sensitivity is proposed, its dependence on design parameters is outlined, and recommendations for their selection are provided. The theoretical results are confirmed by an experiment, carried out with the use of an industrial robot.

Keywords

Accuracy of measurement, sensitivity, distance measurement, design parameters, machine vision, laser triangulation rangefinder

Introduction

Laser triangulation rangefinders (hereinafter – LTRs) are broadly used in various technical applications requiring distance measurements [2,7,8], for example, in position estimation [6] and surface scanning [3,4,5]. As of now, there is a variety of LTRs' manufacturers presented on the market, offering a wide range of models that cover the needs of the majority of practical applications [9, 10]. At the same time, in certain cases, the use of commercial LTRs is impossible or impractical for reasons associated, for instance, with the necessity for a specific configuration of an LTR [1,11] or an integration with visual control devices of the measurement zone [12], as well as in cases of measuring reflective and semitransparent surfaces and surfaces with complex curvature [13]. Besides, there are tasks for which the accuracy of commercial devices may be excessive, and their cost is extremely high [14,15]. In customized solutions, additional systems of mirrors [16], various numbers and types of photo matrices [11,12,16,17,18], different lasers by the type of projection [14,15] and radiation range [13,17] can be applied.

Problems arising in the development of LTRs, as well as approaches aimed at improving the precision of such measurement systems, can be provisionally divided into optical and design groupings. The first set includes actual features of implementation of the measuring system's optical part (lenses, mirrors, focal length, etc.) [4,15,16], the resolution of the recording matrix [22], consideration of its distortion [15] and features of the speckle pattern's registration [19], including cases of projecting a laser onto various surfaces [11, 20]. The design characteristics of LTRs include three main parameters, which are set geometrically – the viewing angle of the camera, the tilt and displacement of its optical axis relative to the laser axis. Exactly these parameters determine the dimensions of a measuring system and its operating range, and also have a direct impact on the measurement accuracy [11, 12, 13].

In the currently relevant papers which study the selection of design parameters of LTRs, the authors indicate the correlation of these parameters with the operating range [11, 13, 22] but cover just some aspects of their impact on a pattern of a sensitivity distribution; in particular, they note a quadratic decrease in sensitivity when distancing an object from a measurement system [4,21]. In the given article, these issues are investigated in more depth.

1. Design parameters of the LTR and their variability

* This work was financially supported by the Ministry of Education and Science of the Russian Federation [state contract 02.G25.31.0348].

Figure 1 demonstrates an outline of the measurement system studied in the article. It is described by the camera viewing angle β, its displacement b relative to the laser source (this displacement is named *baseline*), and the camera tilt angle α. The combination of these design parameters determines the working range of the measurement system, the boundaries of which are indicated in the figure z_{min} and z_{max}. This range is defined by the field of view of the laser projection on the controlled surface in the camera view.

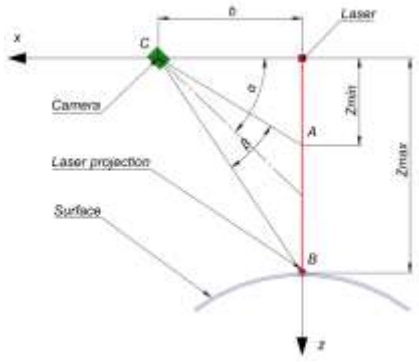

Fig. 1. The outline of the LTR

Expressing the cosine of the camera viewing angle β in terms of the scalar product of the vectors $\overline{CA} = (b, z_{min})$ and $\overline{CB} = (b, z_{max})$, the equation (1) linking primary design parameters of the measurement system is formulated as follows:

$$b^2 + z_{min} \cdot z_{max} = \\ = \sqrt{b^2 + z_{min}{}^2} \cdot \sqrt{b^2 + z_{max}{}^2} \cdot \cos\beta. \quad (1)$$

In this case, the camera tilt angle α turns out to be a dependent parameter, which can be determined as follows:

$$\alpha = \operatorname{atan}\left(\frac{z_{min}}{b}\right) + \frac{\beta}{2}. \quad (2)$$

To illustrate the equation (1), Figure 2 is considered. It reveals curves plotted for three different ranges (z_{min}, z_{max}). Each of the presented curves forms a multitude of combinations of design parameters of the measurement system, corresponding to a given operating range.

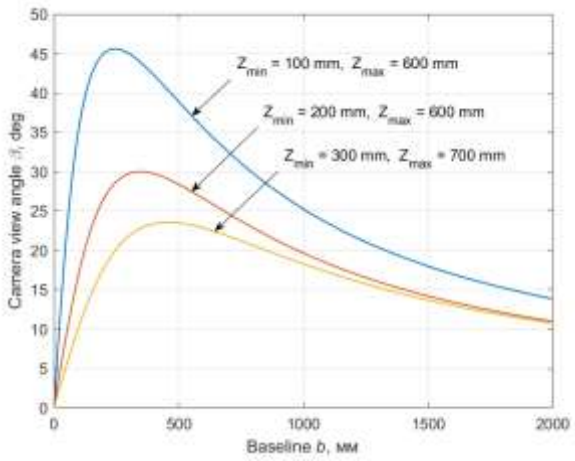

Fig. 2. Variability of solutions in selection of design parameters

The pattern of dependencies shown in Figure 2 is preserved for other operating ranges as well. As the baseline b increases, the camera viewing angle β initially increases monotonically to the maximum value β_{max} and then monotonically decreases, asymptotically tending to zero. It can be demonstrated that the tilt angle of the camera α decreases all the time, whereas at the moment when the camera angle reaches the maximum value β_{max}, the value of the baseline b reaches the value of

$$b_{max} = z_{min}\sqrt{\frac{z_{max}}{z_{min}}}, \quad (3)$$

and the tilt angle of the camera α is always 45 degrees.

For the convenience of the subsequent presentation, the set of solutions with $\alpha > 45°$ which corresponds to $b \in (0, b_{max})$, will be named a measurement system with a narrow baseline. In the case of $\alpha < 45°$ and $b > b_{max}$, a system with a wide baseline is implied.

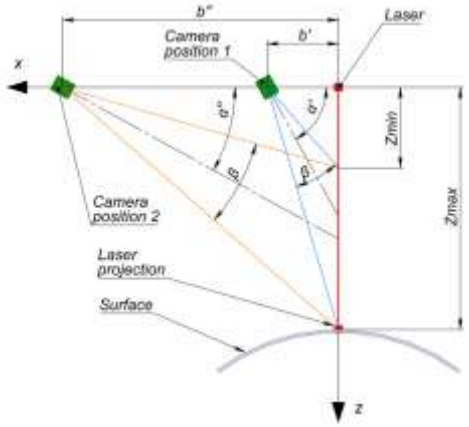

Fig. 3. Examples of measurement systems with narrow and wide baselines

To illustrate the variability of design solutions for the implementation in an LTR, Figure 3 outlines two measurement systems constructed on the basis of cameras with the same viewing angle β, which possess the same operating range (z_{min}, z_{max}). The presented systems differ in baselines b' and b'' , and camera tilt angles α' and α''. It can be noted that in accordance with the accepted terminology, the first system refers to systems with a narrow baseline, and the second one – to systems with a wide baseline.

2. Sensitivity profile of the measurement system

In the previous section, it was highlighted that for any range, there are multiple configurations of the LTR's design parameters. In this section, the effect of opting for these parameters on the accuracy of the measurement system will be studied. To do this, the dependence of the position of the laser projection u in the camera frame on the distance to the surface z is formulated:

$$u(z) = \frac{f \cdot \left(\mathrm{tg}\alpha - \frac{z}{b}\right)}{\frac{z \cdot \mathrm{tg}\alpha}{b} + 1}, \quad (4)$$

where f is the focal factor which depends on the resolution of the photosensitive matrix and the focal length of the optical system. Differentiating equation (4) with respect to z, the ratio of the position change of the beam projection in the camera frame to the change in the distance to the object is obtained:

$$s(z) = \frac{du(z)}{dz} = \frac{b \cdot f \cdot (\mathrm{tg}^2\alpha + 1)}{(b + z \cdot \mathrm{tg}\alpha)^2}. \quad (5)$$

Equation (5) characterizes the dependence of the measurement system's sensitivity on the distance to the object z. This dependence will be named a sensitivity profile of the measuring system. Figure 4 demonstrates, as an instance, sensitivity profiles of two measurement systems covered earlier in Figure 3. The systems have the same operating range $z_{min} = 100$ mm, $z_{max} = 300$ mm, and the camera viewing angle $\beta = 20°$, $f = 1400$. In this case, the baselines and tilt angles of the cameras that satisfy (1) will have the value: for the system with a narrow baseline: $b = 62$ mm, $\alpha = 68.2°$; for the system with a wide baseline: $b = 489$ mm, $\alpha = 21.6°$. The figure illustrates how much the sensitivity of an LTR can change over the operating range, and how strongly this dependence can vary from the configuration of a measurement system: the sensitivity of a measurement system with a short baseline at the edges of the operating range differs by more than six times, while in a system with a wide baseline this difference does not exceed 30%.

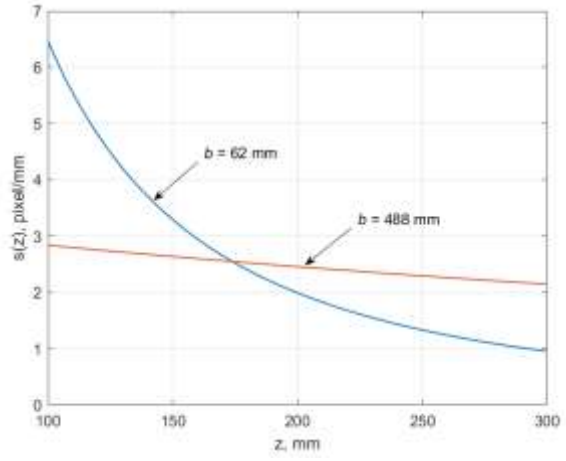

Fig. 4. Examples of sensitivity profiles

It is important to note that integral sensitivity

$$h = \int_{z_{min}}^{z_{max}} s(z)dz = u(z_{max}) - u(z_{min}) \quad (6)$$

in the systems under consideration is the same, but due to the non-uniformity of the $s(z)$ profile, the sensitivity of a system with a narrow baseline at the far border of the working range z_{max} is more than twice as lower. It is worth noticing that the opposite situation is observed at the near border of the working range z_{min}. However, from the point of view of guaranteed measurement accuracy over the entire operating range, a measurement system with a wide baseline, having a profile with a more uniform sensitivity, turns out to be more preferable here.

Thus, the selection of design parameters of an LTR should be guided by the preferred sensitivity profile of a measurement system. In the framework of this study, a profile uniformity is proceeded as preferable. For its quantitative assessment, the criterion is introduced:

$$q = \frac{s(z_{max})}{s(z_{min})} = \left(\frac{b + z_{min} \cdot \mathrm{tg}\alpha}{b + z_{max} \cdot \mathrm{tg}\alpha}\right)^2, \quad (7)$$

which is the ratio of sensitivities of the measurement system at the edges of the working range. Criterion (7) will be named the ratio of the uniformity of the sensitivity profile. The closer the ratio q is to one, the more uniform the profile is (e.g., for sensitivity profiles of narrow and wide baseline systems shown in Figure 4 (Figure 3), this ratio is 0.15 and 0.76, respectively).

3. Dependence of the sensitivity of the LTR on the design parameters

Analyzing expression (7) for the ratio of uniformity q, it is noticeable that it depends not on the absolute values of z_{min}, z_{max}, and b, but on their ratios. Indeed, with proportional scaling of the measurement system, when all angles and correlations between design parameters are preserved, the character of nonlinearity of expression (5) is also preserved.

The baseline b included in expression (7), according to expression (1), depends on the boundaries of the working range z_{min}, z_{max}, and the camera viewing angle β, and can be expressed through them. Thus, in terms of the uniformity of the sensitivity profile q, any LTR designed according to Figure 1 can be described by two parameters independent of the scale of the measurement system: the ratio of the boundaries of the working range

$$r = \frac{z_{max}}{z_{min}} \quad (8)$$

and the camera viewing angle β. Figure 6 represents the dependences of the uniformity ratio of the sensitivity profile q on these parameters for measurement systems with narrow and wide baselines. Note that the areas of construction of heat maps have a border which sets the maximum viewing angle α for each ratio r. The same maximum angle was previously underlined on the curves in Figure 2. This is the limiting angle at which the measurement system can be configured so that the camera's field of view is not wider than the operating range. Violation of this condition is possible in practice, but it leads to incomplete use of the photosensitive area of the matrix and a decrease in the resolution of the measurement system. Such solutions are not considered in the study.

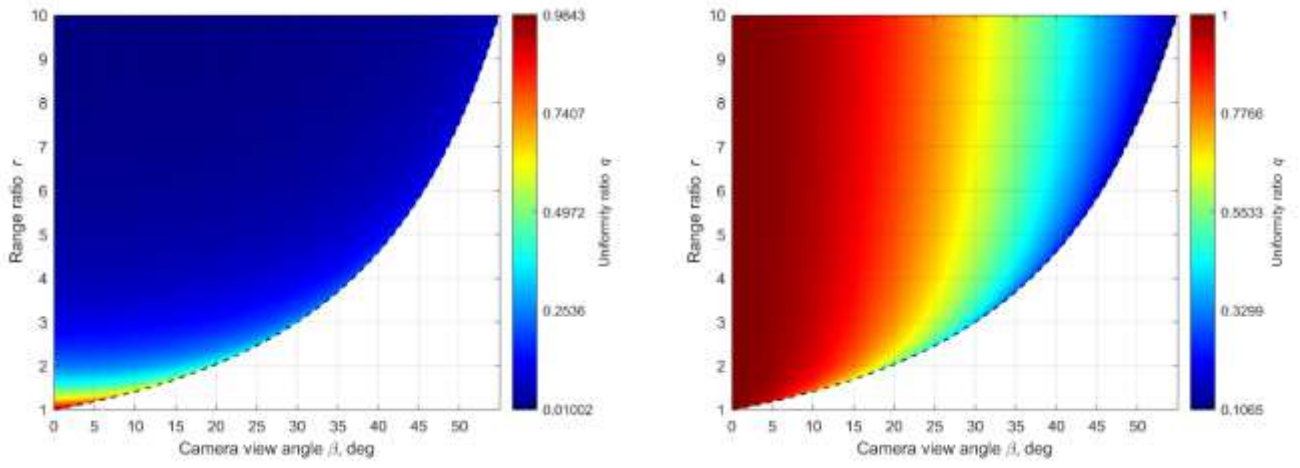

a) b)

Fig. 6. Heat maps of the uniformity ratio of the sensitivity profile for measurement systems with a narrow (a) and wide (b) baselines

Figure 6 highlights that measuring systems with a wide baseline generally possess a more uniform sensitivity profile. For systems with a narrow baseline, the ratio q increases uniformly as the ratio r decreases, whereas for systems with a wide baseline, the ratio q increases uniformly as the viewing angle β decreases. Figure 7 reveals the change of the camera tilt angle α in this case.

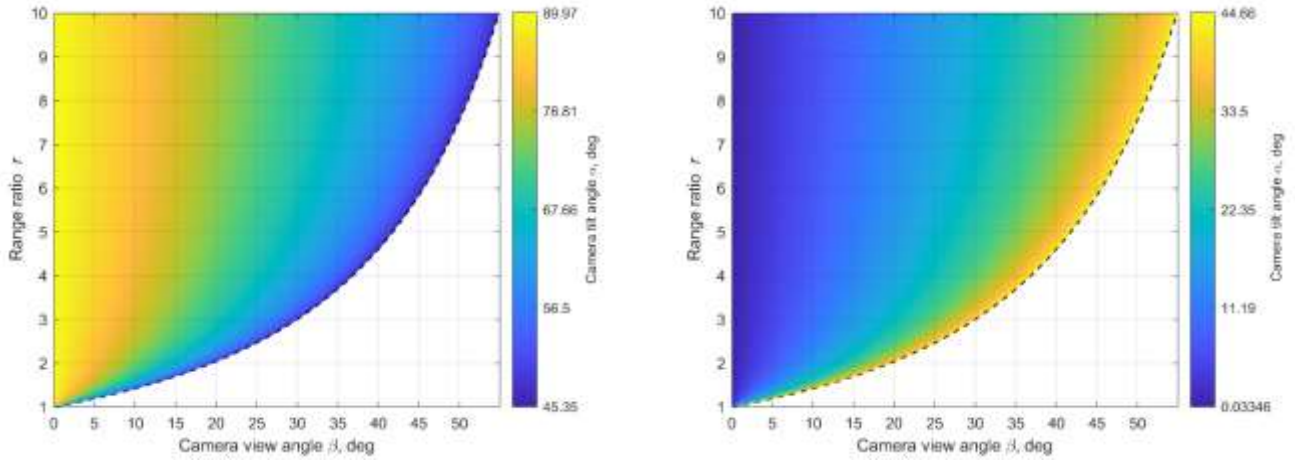

a) b)

Fig. 7. Heat maps of the camera tilt angle for measurement systems with a narrow (a) and wide (b) baselines

It should be noted here that the baseline of the measuring system b is proportional to the ratio $\frac{z_{max}}{\sin\alpha}$, and at small angles α it can increase critically. This situation, in particular, arises in systems with a wide baseline in the area of small camera viewing angles.

Therefore, when selecting the design parameters of the LTR, it is advisable to be guided by the required ratio of the boundaries of the operating range *r*. For small values of *r*, it is recommended to consider configurations of measurement systems with a narrow baseline and a small camera viewing angle. If the ratio *r* is significant, then attention should be paid to measurement systems with a wide baseline, and the larger the baseline *b* is, the more uniform the sensitivity profile will be for the system.

4. Experiment

Until now, the work has been focused on the sensitivity of measurement systems and its distribution within the operating range. This quality is inherent in all measurement systems of the class under consideration, regardless of the features of their hardware implementation.

The sensitivity $s(z)$, determined by equation (5), sets the number of pixels by which the projection of the beam in the camera frame is shifted when the distance *z* changes by 1 mm. Thus, the resulting accuracy of the measuring system depends both on the sensitivity $s(z)$ and on the actual registration accuracy of the position of the laser beam projection in the camera frame. This section is devoted to an experimental study of the accuracy of recording the beam position in the frame, its dependence on distance and the impact on the resulting accuracy of the measurement system.

Experiments were performed using a Logitech HD Webcam C270 camera with a vertical matrix expansion of 720 pixels and an experimentally determined viewing angle $\beta = 37.35°$. Two measurement systems with different working ranges are considered: $Z_1 \in [50, 450]$ mm and $Z_2 \in [100, 500]$ mm. It can be noticed that in both cases the ranges have the same width, but the ratio of their boundary values is significantly different: in the first case $r = 9$, in the second one $r = 5$. Calculated values of baselines and camera tilt angles (obtained via equation (1) and rounded up) are: $b = 47$ mm, $\alpha = 65°$, and $b = 125$ mm, $\alpha = 57°$, respectively. Both design solutions refer to systems with a narrow baseline. Note that, according to (7), the considered systems have $q = 0.023$ and $q = 0.097$, i.e. their sensitivity ratios at the edges of the range differ several times.

The experiment was carried out using an industrial robot KUKA KR10 R900. A photo of the experimental setup is revealed in Figure 8. The measurement module is placed on the flange of the robot and moves vertically with a constant speed of 5 mm/s in a given range. This allows a controlled change in the distance *z* to the projection of the beam on the surface.

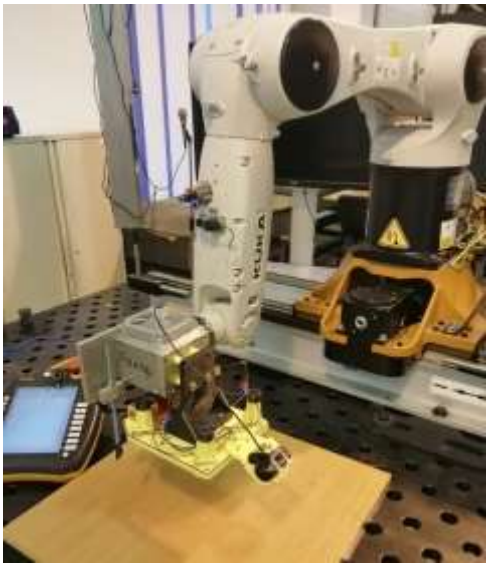

Fig. 8. Photo of the experimental installation

Registration of the position of the laser beam projection in the camera frame is performed via filtering the image by the brightness threshold. The coordinate of the projection center of the spot on the image is determined by calculating its center of mass. As z increases and the ray projection move away from the camera, its size in the frame decreases. Figure 9 shows the types of the laser beam at the edges of the Z_1 range in the form of image fragments of the same size 50×50 pixels.

a)  b) 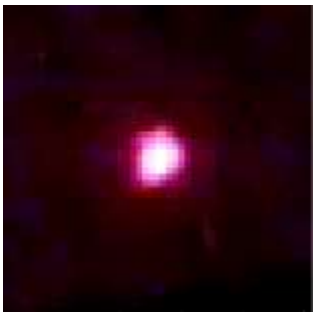

Fig. 9. Laser beam projection images for a) $z = 50$ mm; b) $z = 450$ mm

Figure 10 demonstrates the experimental dependences of the position of the laser beam projection in the frame on the distance to the surface for the considered measurement systems with the working ranges Z_1 and Z_2.

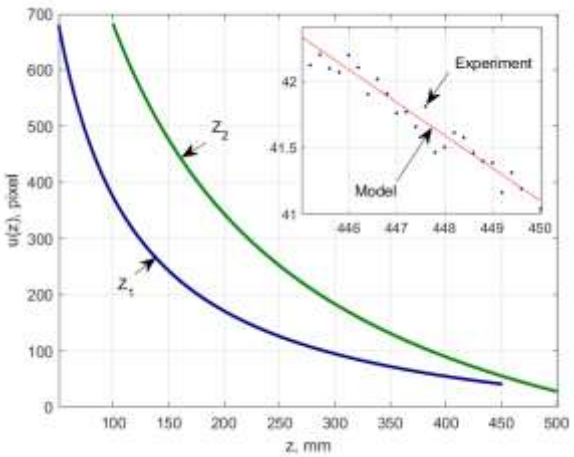

Fig. 10. Dependences of the projection of the laser beam position in the frame on the distance z

The experimental data $\tilde{u}(z)$ presented in the figure is combined with the corrected model dependences $u'(z)$. In the scale of the figure their graphs coincided, therefore the figure contains an enlarged fragment. Correction of the model data was required due to errors in manufacturing and installing the elements of the measuring module and the presence of camera distortion.

As an estimate of the error in determining the position of the laser beam projection $e_p(z)$, the difference between the corresponding model $u'(z)$ and experimental $\tilde{u}(z)$ coordinates will be used:

$$e_p(z) = u'(z) - \tilde{u}(z). \tag{9}$$

Figure 11 represents an estimate of the error in registering the position of the of the laser projection for a measurement system with an operating range of Z_1. For the convenience of analyzing the presented data, this figure also shows the threshold obtained on the basis of the moving standard deviation

$$E_i = \pm 2 \sqrt{\frac{1}{n} \sum_{j=i-m}^{j=i+m} e_j^2}, \tag{10}$$

where $n = 2m + 1$ is the width of the sliding window, and e is an element of the time series. In accordance with the properties of the normal distribution, the threshold E, which is the doubled value of the standard deviation, determines the tier that a random signal will not exceed in 95% of cases.

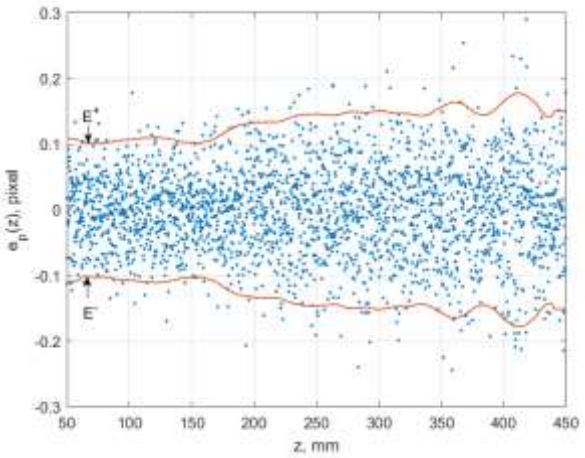

Fig. 11. Error estimation in determining the position of the laser beam projection on the image for the range Z_1

Figure 11 demonstrates that the error of the algorithm used for determining the position of the laser spot is 0.1 ... 0.2 pixels. This is achieved by generalizing over the entire spot area (see Figure 9). In this case, the experiment did not reveal a critical dependence of the error in determining the position of the spot on its area, although in general, the error $e_p(z)$ increases when moving away from the camera.

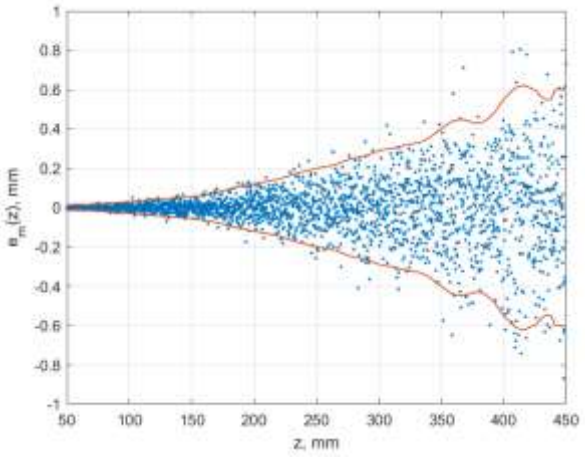

Fig. 12. Estimation of the distance measurement error for the system with the working range Z_1

An estimate of the error in measuring the distance $e_m(z)$ is obtained by adjusting the error $e_p(z)$ for the sensitivity profile $s(z)$:

$$e_m(z) = \frac{e_p(z)}{s(z)}. \tag{11}$$

Figure 12 represents an estimate of the distance measurement error for a system with an operating range of Z_1. The figure below illustrates a measurement system with extremely high sensitivity non-uniformity. For comparison, Figure 13 shows the estimate of the distance measurement error in a system with an operating range of Z_2.

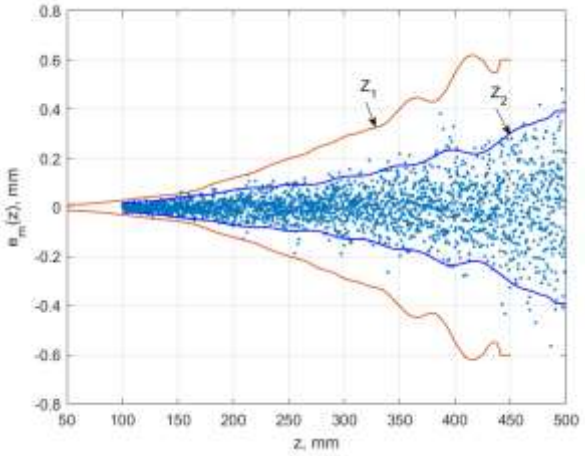

Fig. 13. Estimation of the distance measurement error for the system with the working range Z_2

For convenience of comparison, Figure 13 illustrates a copy of the threshold *E* of the measurement system with the working range Z_1. The figure reveals that over most of the operating range, the systems possess significantly different accuracy. The difference is about twice as much. Simultaneously, the systems have the same hardware implementation and the same working range width of 400 mm. Figure 13 clearly represents the influence of selecting design parameters of the measurement system on its accuracy.

Conclusion

The study identifies a group of design parameters of the LTR which determine the operating range of the measurement system and impact the distribution of its sensitivity. The correlation between design parameters and their variability is illustrated. The influence of design parameters on the non-uniformity of the sensitivity of the measurement system is outlined and formalized. It was determined that the key role in this influence is played by the ratio of the operating range's boundary values. A quantitative criterion for assessing the uniformity of sensitivity is proposed, its dependences on design parameters are provided, and recommendations for their selection are listed. The experiment using an industrial robot was carried out, during which the dependence of the error in registering the position of a laser beam projection on its distance to the camera was investigated. It was found that this error is estimated at approximately 0.1 ... 0.2 pixels and depends slightly on the distance to the camera. Based on experimental data, estimates of the distance measurement accuracy for systems with different sensitivity uniformity indicators are obtained.

References

[1] I. V. Filonov, K. V. Zmeu, B. S. Notkin and I. A. Baranchugov, "Laser Measuring System for Tool and Surface Relative Positioning When Robotic Processing," 2020 International Multi-Conference on Industrial Engineering and Modern Technologies (FarEastCon), Vladivostok, 2020, pp. 1-5

[2] Peng Li, Xiangpeng Liu, "Common Sensors in Industrial Robots: A Review", IOP Conf. Series, 2019 [2019 Journal of Physics: Conf. Series 1267(2019)012036]

[3] Robert Bogue, "Three-dimensional measurements: a review of technologies and applications", Emerald Insight, 2010

[4] Junhua Sun, Jie Zhang, Zhen Liu, Guangjun Zhang, "A vision measurements model of laser displacement sensor and its calibration method", Elsevier, 2013

[5] Johannes Schlarp, Ernst Csencsics, Georg Schitter, "Design and evaluation of an integrated scanning laser triangulation sensor", Elsevier, 2020

[6] Ahmed Hussein, Pablo Marin-Plaza, David Martin, Arturo de la Escalera, Jose Maria Armingol, "Autonomous Off-Road Navigation using Stereo-Vision and Laser-Rangefinder Fusion for Outdoor Obstacles Detection", IEEE, 2016 [2016 IEEE Intelligent Vehicles Symposium (IV)]

[7] Young Soo Suh, "Laser Sensors for Displacement, Distance and Position", MDPI Sensors,2019

[8] Young Soo Suh, "3D metrology using a collaborative robot with a laser triangulation sensor", Elsevier,2017

[9] Bin Sun, Bing Li, "Laser Displacement Sensor in the Application of Aero-Engine Blade Measurement", IEEE Sensors Journal, 2016

[10] Matthew Kuester, Nanyaporn Intaratep, Aurelien Borgoltz, "Laser Displacement Sensors for Wind Tunnel Model Position Measurements", MDPI Sensors, 2018

[11] Chris Cain, Alexander Leonessa, "Laser Based Rangefinder for Underwater Applications", IEEE, 2012 [2012 American Control Conference]

[12] Fitri Utaminingrum, Tri Astoto Kurniawan, M Ali Fauzi, Rizal Maulana, Dahnial Syauqy, Randy Cahya Wihandika, Yuita Arum Sari, Putra Pandu Adikara "A Laser-Vision based Obstacle Detection and Distance Estimation for Smart Wheelchair Navigation", IEEE, 2016 [2016 IEEE International Conference on Signal and Image Processing]

[13] Kazuki Kasahara, Takahiro Ugajin, Mitsuri Baba "3D Shape Measurement of Translucent Objects Using Laser Rangefinder", IEEE, 2017 [2017 56th Annual Conference of the Society of Instrument and Control Engineers of Japan (SICE)]

[14] Kurt Konolige, Joseph Augenbraum, Nick Donaldson, Charles Fiebig, Pankaj Shan "A Low-Cost Laser Distance Sensor", IEEE, 2008 [2017 International Conference on Robotics and Automation]

[15] Xinzheng Zhang, Yi Yang, Zhong Liu, Jianfen Zhang "An improved sensor framework of mono-cam based laser rangefinder", Elsevier,2013

[16] Dawei Ding, Zhengcai Zhao, Rui Huang, Chenwei Dai, Zinquan Zhang, Taorui Xu, Yucan Fu "Error Modeling and Path Planning for Freeform Surfaces by Laser Triangulation On-Machine Measurement", IEEE, 2021 [2021 IEEE Transactions on Instrumentation and Measurement]

[17] M.M. Bykov, V.S. Tyurin "Increase of measurement accuracy of distances by laser rangefinder with adaptive threshold", IEEE, 2005 [2005 Proceedings of CAOL 2005. Second International Conference on Advanced Optoelectronics and Lasers]

[18] Francois Blais "Review of 20 years of range sensor development", Journal of Electronic Imaging 13(1), pp. 231-240, 2004

[19] Rejean Baribeau and Marc Rioux "Influence of speckle on laser range finders", Applied Optics Vol. 30, No. 20, pp. 2873-2878, 1991

[20] Mehdi Daneshpanah, Kevin Harding "Surface sensitivity reduction in laser triangulation sensors", SPIE, 2011 [2011 Dimensional Optical Metrology and Inspection for Practical Applications]

[21] Chensong Dong "A regression model for analysing the non-linearity of laser triangulation probes", Springer, 2011 [2012 The International Journal of Advanced Manufacturing Technology]

[22] Chensong Dong "Accuracy and Resolution of Kinect Depth Data for Indoor Mapping Applications", MDPI Sensors, 2012